Thermal Protection System Mass Estimating Relationships For Blunt-Body, Earth Entry Spacecraft

Steven A. Sepka[1]
ERC Incorporated, Moffett Field, CA, 94035

Jamshid A. Samareh[2]
NASA Langley Research Center Hampton, VA 23681

Mass estimating relationships (MERs) are developed to predict the amount of thermal protection system (TPS) necessary for safe Earth entry for blunt-body spacecraft using simple correlations that are non-ITAR and closely match estimates from NASA's high-fidelity ablation modeling tool, the Fully Implicit Ablation and Thermal Analysis Program (FIAT). These MERs provide a first order estimate for rapid feasibility studies. There are 840 different trajectories considered in this study, and each TPS MER has a peak heating limit. MERs for the vehicle forebody include the ablators Phenolic Impregnated Carbon Ablator (PICA) and Carbon Phenolic atop Advanced Carbon-Carbon. For the aftbody, the materials are Silicone Impregnated Reusable Ceramic Ablator (SIRCA), Acusil II, SLA-561V, and LI-900. The MERs are accurate to within 14% (at one standard deviation) of FIAT prediction, and the most any MER can under predict FIAT TPS thickness is 18.7%. This work focuses on the development of these MERs, the resulting equations, model limitations, and model accuracy.

Nomenclature

a,b	=	power-law fit coefficients
CW	=	cold wall
HL	=	total heat load, J/cm^2
MER	=	mass estimating relationship
P	=	surface pressure, Pa
SD	=	standard deviation
TH	=	TPS thickness, cm
TPS	=	thermal protection system
V	=	entry velocity, km/s
V_∞	=	free stream velocity, km/s
ρ_∞	=	free stream density, kg/m^3

I. Introduction

A multidisciplinary, integrated tool called the "Multi Mission System Analysis for Planetary Entry Descent and Landing," also known as M-SAPE[1], is being developed as part of the Entry Vehicle Technology project under NASA's In-Space Technology program. Part of M-SAPE's application requires the development of parametric mass estimating relationships (MERs) to determine a vehicle's required Thermal Protection System (TPS) for safe Earth entry. For this analysis, the heat shield is made of a uniform thickness TPS, and the resulting MERs determine the pre-flight mass of the TPS.

The analysis and design of an Earth Entry Vehicle is very multidisciplinary in nature, requiring the application of aerodynamics, aerothermodynamics, and material response. For a typical re-entry problem, computational aerothermodynamics is used to determine the flow conditions around the vehicle, including heating to its surface. Once the entry environment is known, then a TPS material response is modeled to determine the material thickness

[1] Senior Research Scientist, NASA-Ames Research Center, Thermal Protection Materials Branch (Code TSM) MS-234-1, Moffett Field, CA, 94035.
[2] Senior Aerospace Research Engineer, Vehicle Analysis Branch.

necessary to keep the bond line temperature below a specified value. It is also important to know the amount of surface recession, if any. The traditional approach for this coupled problem would be to first use a high fidelity computational fluid dynamics code such as the Data Parallel Line Relaxation[2] (DPLR) code or the Langley Aeroheating Upwind Relaxation Algorithm[3] (LAURA) for the aerothermal component. Then for TPS response one could use the Fully Implicit Ablation and Thermal Response[4] (FIAT) code, the Charring Material Thermal Response and Ablation Program[5] (CMA), the Charring Ablating Thermal Protection Implicit System Solver[6] (CHAR), or the Standard Ablation Program[7] (STAB). However, this coupled approach usually has a very slow turnaround time and is highly dependent upon analyst availability. To circumvent these issues, M-SAPE employs correlations to bypass these codes with as minimal a loss in accuracy as possible.

For the vehicle forebody stagnation point, M-SAPE uses the Sutton - Graves[8] (SG) correlation for convective heating and the Tauber - Sutton[9] correlation for radiative heating. To date, however, no correlations based on high-fidelity FIAT modeling are known. As a result, the current work is to develop FIAT-based MERs that match FIAT prediction as closely as possible. Six MERs are developed. For the vehicle forebody the ablative materials are Phenolic Impregnated Carbon Ablator[10] (PICA) and Carbon Phenolic[11] atop Advanced Carbon-Carbon. For the vehicle aftbody the materials are Silcone Impregnated Reusable Ceramic Ablator[12] (SIRCA), Acusil[13] II, SLA-561V, and LI-900. As will be shown, the MERs are accurate to FIAT prediction within 18.7% at one standard deviation. For these MERs, no margins have been added to the TPS thickness.

Using these MERs, M-SAPE can now perform rapid trade studies involving entry velocity, ballistic coefficient, vehicle geometry, entry flight path angle, etc. for required TPS thickness. Design turnaround times for a possible Earth entry configuration are reduced from weeks to hours.

II. MER Development

A. Concern Regarding the Application of MERs

The MERs are statistical correlations developed to predict FIAT output. Each MER has with it a listed accuracy to the FIAT code's prediction, which is the standard deviation of the MER/FIAT ratio over all trajectories.

Each material has a maximum allowable instantaneous heat flux (convective and radiative). M-SAPE has correctly implemented this restriction into its code.

It is emphasized that the MER thickness is not the manufacturing limit, and that substantial margin may be added. For example, Stardust flew with a PICA thickness[14] of 5.816 cm (2.29 inch), which is much greater than its unmargined thickness.

Finally, as for any statistical analysis there exist some trajectories for which the ratio of MER/FIAT prediction can well exceed the listed MER accuracy at one SD. For the present work, the largest possible MER under prediction of FIAT is 18.7%. It is for this reason that full datasets are presented showing the curve fit and MER/FIAT "goodness-of-fit" data. M-SAPE uses these MERs as a rough approximation to determine TPS thickness for flight trajectories of interest, but always maintains that a true high-fidelity analysis is always a requirement for a proposed mission.

B. Flight Trajectory Parameters

Found in Table 1 is information on the flight trajectory parameters used for this study.

Table 1. Flight trajectories considered for the MERs

Flight Trajectory Parameter	Range of Values	Resolution
Entry Velocity [km/s]	10-16	1
Entry Flight Path Angle [abs. deg.]	5-25	5
Ballistic Coefficient [kg/m^2]	41.95 – 128.74	15.5 (max)
Total number of trajectories	840	-

Here, resolution is defined as a parameter's smallest step-size

C. Vehicle Geometry Parameters

Details of the vehicle geometry are given in Table 2.

Table 2. Vehicle Geometry

	min	max
Nose Radius [m]	0.352	0.352
Vehicle Diameter [m]	0.75	2.25
Vehicle Mass [kg]	16.31	158.7
Payload Mass [kg]	5	30

D. FIAT modeling constraints

FIAT analysis of each trajectory uses the following constraints:

- The maximum temperature at the bottom face of the top material (bond line) is 250°C.
- The back face of the material stackup is adiabatic.
- The surrounding environment is at 21.3°C, for radiation calculations from the spacecraft surface.
- 1D planar geometry
- No margins are added to the thickness
- FIAT v3.0

It should be noted that FIAT is a 1D code and is most applicable for regions that are planar, cylindrical, or spherical sections. Examples of regions such as these are at the stagnation point, along the flank, or any other acreage location. For regions that do change shape quickly, such as at the shoulder, a material response code like TITAN,[15] 3dFIAT, or CHAR is more appropriate because it includes 2D or 3D effects. In addition, PICA's heat conduction is orthotropic, which also necessitates the use of multi-dimensional codes along regions of the heat shield that change shape quickly. Shown in Table 3 are the ranges of trajectory heating rates, heat loads, and surface pressures used in FIAT analysis of the 840 flight trajectories. The data shown in this table are prior to MER development.

Table 3. Surface heating, heat load, and surface pressures found by running FIAT over all trajectories.

	Forebody	Aftbody
Maximum heat flux [W/cm^2]	151 – 3767	2.3 – 58.1
Heat Load [J/cm^2]	3855 – 34453	59.4 – 531.0
Maximum pressure, atm	0.03 – 3.182	0.005 – 3.182

E. Methodology

1. MER Formulation

The variables considered to create the MERs included peak heat flux, peak surface pressure, heat load, ballistic coefficient, entry velocity, and entry flight path angle. To determine which of these variables to use, sensitivity studies were conducted by plotting the value of each variable against required TPS thickness for all trajectories. Viewing these scatter plots and calculating correlation coefficients determined if any correlation or sensitivity existed. For this work, heat load and entry velocity were chosen for the MER correlations. We have selected a ratio of heat load over square of velocity as the correlation parameter that represents the ratio of entry thermal energy over entry kinetic energy.

2. Forebody Calculations

The form of the Sutton-Graves relation used by M-SAPE is a cold-wall (CW) convective heat flux. Consequently, the convective heat load used in the MERs is CW. For the radiative heat load, the Tauber-Sutton relation was used to estimate the radiative heating. Surface pressure was found using the momentum equation:

$$P = \rho_\infty V_\infty^2 \tag{1}$$

When FIAT ran through all 840 trajectories, 123 of them were so mild as to produce no recession or ablation for PICA and Carbon Phenolic. For such mild environments, the proper heat shield material is an insulator rather than an ablator. As a result, these mild trajectories were not used in the forebody MERs, and the MER minimum thickness was chosen from the first trajectory to cause any ablation. This minimum thickness is enough material to keep the bond line temperature below 250°C for the mild trajectories.

A trajectory's peak heat flux was used to determine if a TPS was applicable. If a trajectory's peak heating exceeded a TPS material's allowed value (see Table 4), then it was discarded and not included in the analysis.

3. Aftbody Calculations

To estimate the aerothermal environment on the aft body, convective heating was found by taking 5% of the forebody stagnation point heating. Radiative heating was ignored, and surface pressure was 50% of the forebody

stagnation point value. Peak heating rates for all trajectories were low enough such that all were used in the formulation of the aft body MERs.

F. Summary of Results

The results are summarized in Table 4. A discussion of these results, how they were obtained, and their accuracy is given in Section III.

Table 4. Summary of the results.

	PICA	CP/ACC	SIRCA	Acusil II	LI-900	SLA-561V
Recession [cm]	0.60 – 1.15	0.0002 – 0.141	none	none	none	none
Accuracy to FIAT (one SD)	6.3%	7.3%	8.5%	7.6%	14.0%	8.5%
Largest possible under prediction (% of FIAT)	11.7	16.6	15.6	15.1	18.7	15.7
Minimum thickness [cm]	3.27	2.27	0.518	0.614	0.686	0.454
Max allowable heat flux, CW [W/cm^2]	1200	30000	100	100	75	100
Thickness [cm]	$1.8696\left(\frac{HL}{V^2}\right)^{0.1873}$	$1.1959\left(\frac{HL}{V^2}\right)^{0.2102}$	$0.5281\left(\frac{HL}{V^2}\right)^{0.5416}$	$0.623\left(\frac{HL}{V^2}\right)^{0.5697}$	$q_{CW} <= 10$ W/cm^2: $0.6961\left(\frac{HL}{V^2}\right)^{0.656}$; $q_{CW} > 10$ W/cm^2: $-0.0306\left(\frac{HL}{V^2}\right)^2+0.5896\left(\frac{HL}{V^2}\right)+0.6739$	$0.0064\left(\frac{HL}{V^2}\right)^2+0.0961\left(\frac{HL}{V^2}\right)+0.3322$

III. Forebody MER Development: PICA and Carbon Phenolic

1. PICA

The material stackup for this MER consists of only PICA, and the FIAT PICA material response model was version 3.3. The MER is given in Eq. 2, and it has a standard deviation of 6.3% to FIAT prediction. Specifics of the correlation model are given in Table 5. Fig. 1 shows the MER fit of the data, and a scatter plot of Goodness of Fit (GoF) with FIAT-predicted TPS thickness is given in Fig. 2. GoF is defined as the ratio of MER to FIAT prediction.

$$TH = 1.8686\left(\frac{HL}{V^2}\right)^{0.1879} \tag{2}$$

Table 5. PICA MER Details

Variable	Values
Maximum allowable heat flux, W/cm^2, CW	1200
Recession, cm	0.134 – 1.153
Accuracy to FIAT at one SD	6.3%
Largest possible under prediction of FIAT (% of FIAT)	11.7
Number of trajectories with no recession	123
Trajectories used for correlation	420
Minimum thickness, cm	3.27

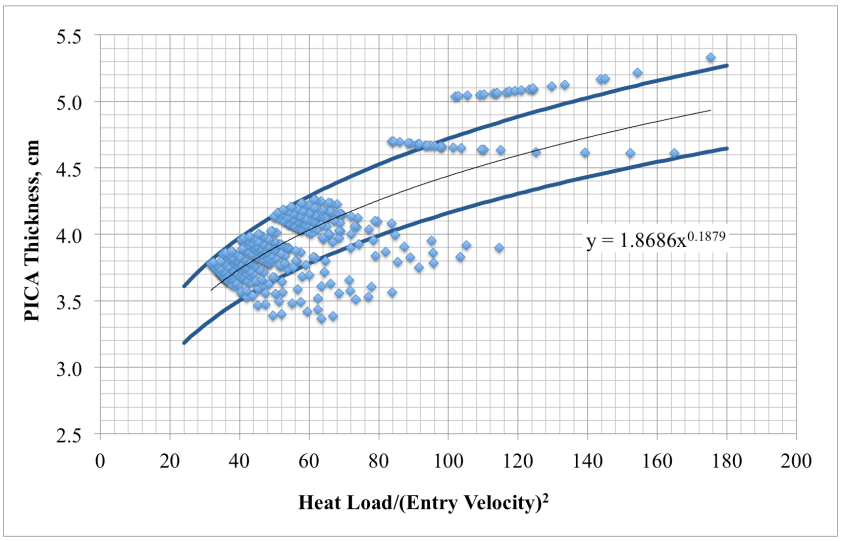

Figure 1. PICA MER banded by 1 standard deviation

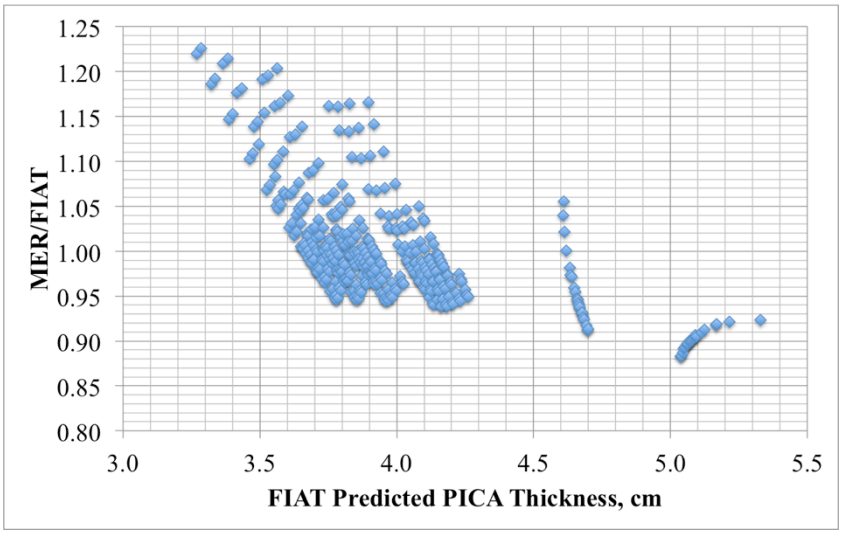

Figure 2. PICA MER Goodness of Fit

2. Carbon Phenolic Atop Advanced Carbon-Carbon 6

The material stackup is given in Table 6. ACC6 is the carrier structure.

Table 6. Material stackup

Material	Thickness, cm
Carbon Phenolic	variable
HT-424 (adhesive)	0.0381
Advanced Carbon-Carbon (ACC) version 6	0.250

This MER is given in Eq. 3, and it has a standard deviation of 7.3% to FIAT prediction. Specifics of the correlation model are given in Table 7. A scatter plot showing the fit to the data is given in Fig. 3, and Fig. 4 shows a scatter plot of GoF with FIAT-predicted TPS thickness.

$$TH = 1.1959\left(\frac{HL}{V^2}\right)^{0.2102} \tag{3}$$

Table 7. Carbon Phenolic atop ACC MER Details

Variable	Values
Maximum allowable CW heat flux, W/cm^2	30000
Recession [cm]	0.0002 – 0.1416
Accuracy to FIAT at one SD	7.3%
Largest possible under prediction of FIAT (% of FIAT)	16.6
Number of FIAT non-convergent trajectories	16
Trajectories with no recession	123
Trajectories used for correlation	701
Minimum thickness, cm	2.266

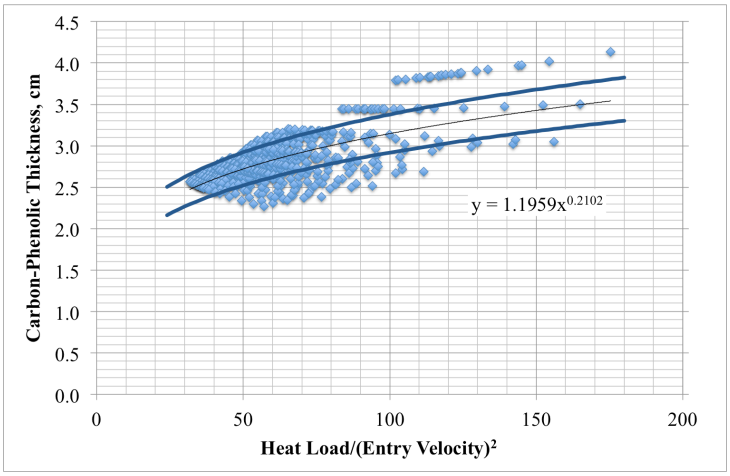

Figure 3. Carbon Phenolic over ACC6 MER banded by 1 standard deviation.

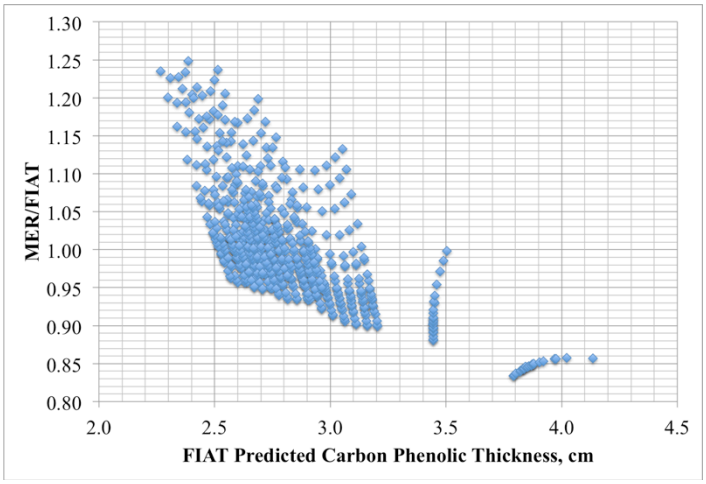

Figure 4. Carbon Phenolic over ACC6 MER GoF.

IV. Vehicle Backshell MERs

1. SIRCA

The material stackup consists only of SIRCA, and the FIAT SIRCA model is version 1.00. The SIRCA MER is given in Eq. 3, and it has a standard deviation of 8.5% to FIAT prediction. Specifics of the MER are given in Table 8. Shown in Fig. 5 is the MER fit of the data, and a scatter plot of Goodness of Fit with FIAT-predicted TPS thickness is given in Fig. 6.

$$TH = 0.5281\left(\frac{HL}{V^2}\right)^{0.5416} \quad (4)$$

Table 8. SIRCA MER Details

Variable	Values
Maximum allowable CW heat flux, W/cm^2	100
Recession, cm	none
Accuracy to FIAT at one SD	7.4%
Largest possible under prediction of FIAT (% of FIAT)	16.6
Trajectories used for correlation	835
Minimum thickness, cm	0.614

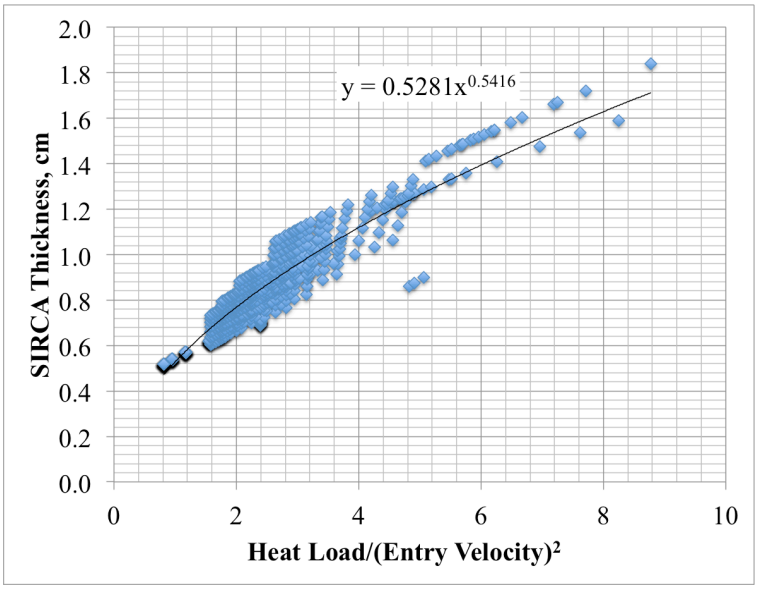

Figure 5. SIRCA MER banded by one standard deviation

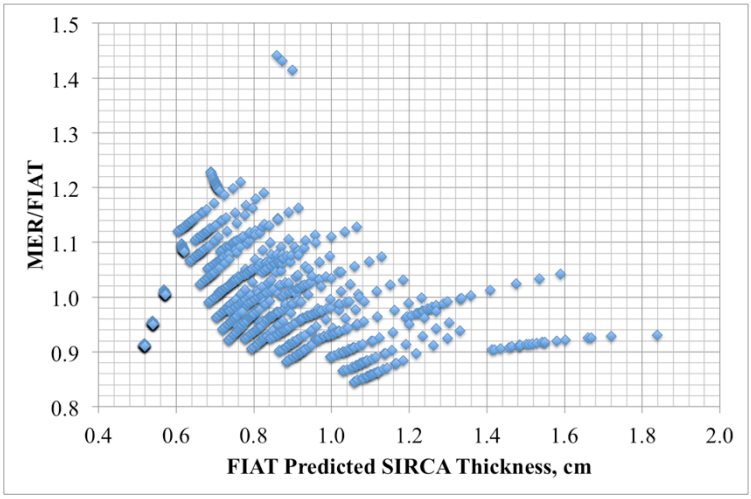

Figure 6. SIRCA MER Goodness of Fit

2. Acusil II

The Acusil II MER is given in Eq. 5, and it has a standard deviation of 7.6% to FIAT prediction. Specifics of the MER are given in Table 9. Shown in Fig. 7 is the MER fit of the data, and a scatter plot of Goodness of Fit with FIAT-predicted TPS thickness is given in Fig. 8.

$$TH = 0.623\left(\frac{HL}{V^2}\right)^{0.5697} \quad (5)$$

Table 9. Acusil II MER Details

Variable	Values
Maximum allowable CW heat flux, W/cm^2	100
Recession, cm	none
Accuracy to FIAT at one SD	7.6%
Largest possible under prediction of FIAT (% of FIAT)	15.1
Trajectories used for correlation	835
Minimum thickness, cm	0.614

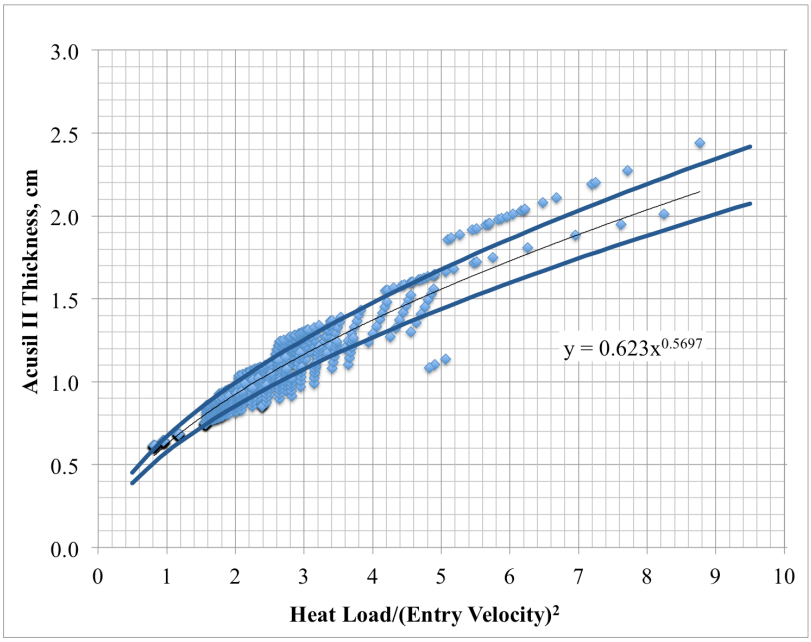

Figure 7. Acusil II MER

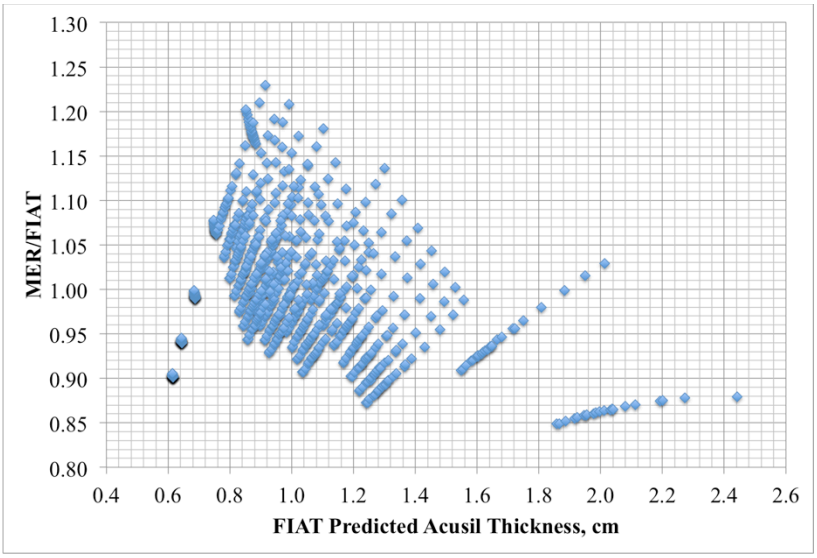

Figure 8. Acusil II MER GoF

3. SLA-561V

The SLA-561V MER is given in Eq. 6, and it has a standard deviation of 8.5% to FIAT prediction. Specifics of the MER are given in Table 10. Shown in Fig. 9 is the MER fit of the data, and a scatter plot of Goodness of Fit with FIAT-predicted TPS thickness is given in Fig. 10.

$$TH = 0.0064\left(\frac{HL}{V^2}\right)^2 + 0.0961\left(\frac{HL}{V^2}\right) + 0.3322 \quad (6)$$

Table 10 SLA-561V MER Details

Variable	Values
Maximum allowable CW heat flux, W/cm^2	100
Recession, cm	none
Accuracy to FIAT at one SD	8.5%
Largest possible under prediction of FIAT (% of FIAT)	15.7
Trajectories used for correlation	834
Minimum thickness, cm	0.454

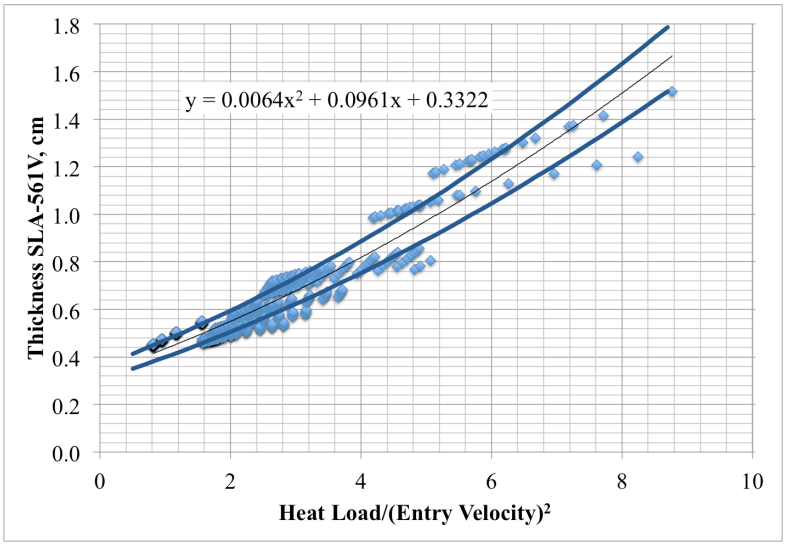

Figure 9. SLA-561V MER

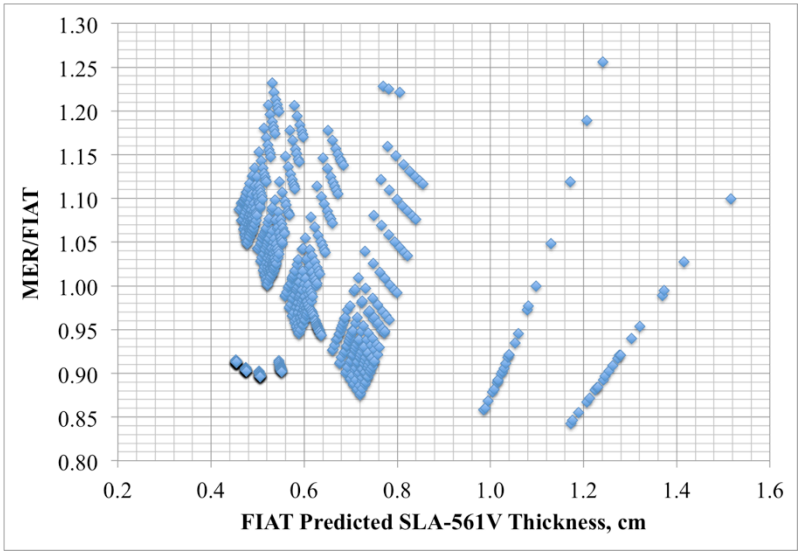

Figure 10. SLA-561V MER Goodness of Fit

4. LI-900

The LI-900 MER is divided by peak heat flux into two equations. They are given in Eq. 7. The MER has a standard deviation of 14.0% to FIAT prediction. Specifics of the MER are given in Table 7. Shown in Fig. 11 is the MER fit of the data, and a scatter plot of Goodness of Fit with FIAT-predicted TPS thickness is given in Fig. 12.

$$\left.\begin{aligned} TH &= 0.6961\left(\frac{HL}{V^2}\right)^{0.656} && q_{cw} \le 10\ \frac{W}{cm^2} \\ TH &= -0.0306\left(\frac{HL}{V^2}\right)^2 + 0.5896\left(\frac{HL}{V^2}\right) + 0.6739 && q_{cw} > 10\ \frac{W}{cm^2} \end{aligned}\right\} \quad (7)$$

Table 1 LI-900 MER Details

Variable	Values
Maximum allowable CW heat flux, W/cm^2	75
Recession, cm	none
Accuracy to FIAT at one SD	14%
Largest possible under prediction of FIAT (% of FIAT)	18.7
Trajectories used for correlation	798
Minimum thickness, cm	0.686

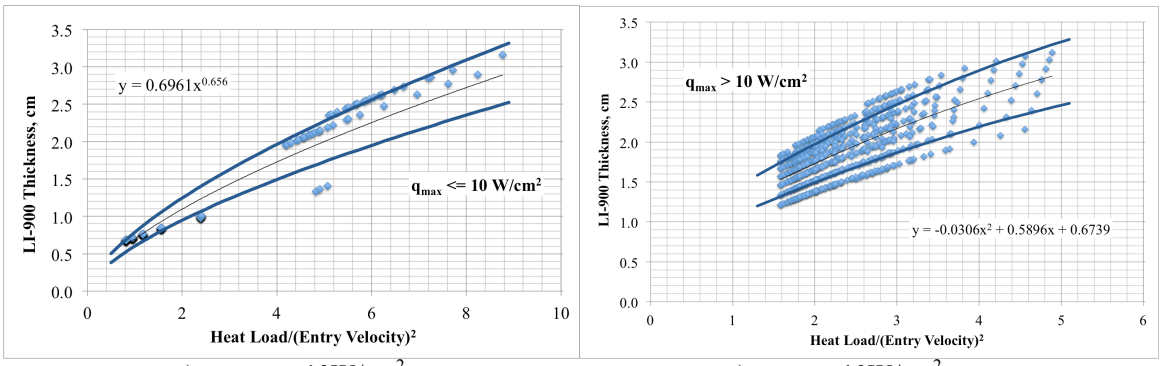

a) qmax <= 10W/cm^2 a) qmax > 10W/cm^2

Figure 11. LI-900 MER

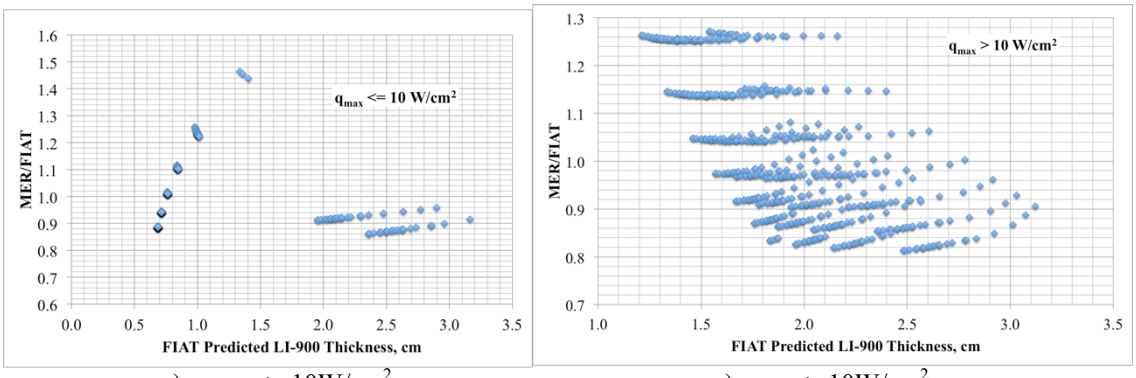

a) qmax <= 10W/cm^2 a) qmax > 10W/cm^2

Figure 12. LI-900 MER Goodness of Fit

V. PICA Arcjet Testing Database

For all the trajectories considered in this work, the highest FIAT predicted heating is over 3700 W/cm^2. PICA has never been tested under such high heating conditions (see Fig. 13), and it is unlikely to survive such a harsh environment. The PICA MER is limited to a cold-wall peak heating of 1200 W/cm^2, and M-SAPE has been configured so that a user is notified if a trajectory exceeds its MERs limit. As a comparative note, it was estimated that a peak heat flux of about 1220 W/cm^2 was experienced on the PICA heat shield of the Stardust[16] capsule.

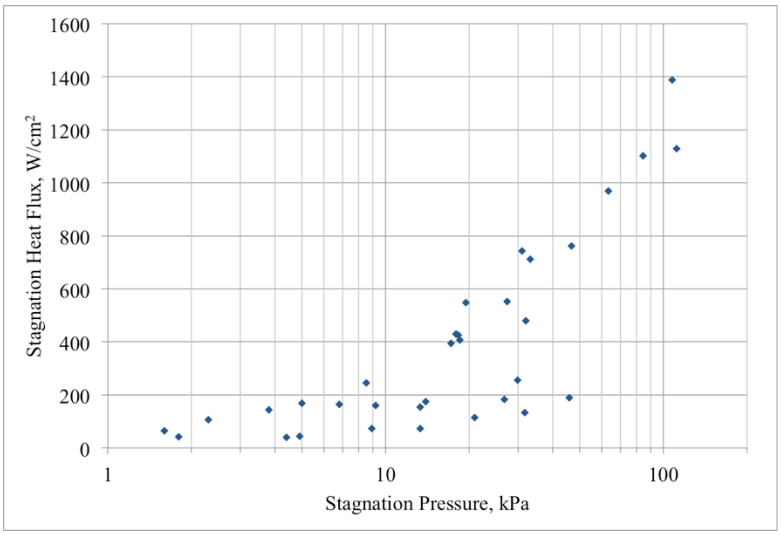

Figure 13. Successful Stagnation Tests of PICA in which no spallation was observed. Heat flux values are cold-wall.

VI. Conclusion

Mass estimating relationships have been presented for the vehicle forebody ablators PICA and Carbon Phenolic atop ACC, and for the backshell materials SIRCA, Acusil II, SLA-561V, and LI-900. These MERs are accurate to FIAT prediction between 7 to 15% at one standard deviation. Applications include quick estimates of TPS mass during early stages of vehicle design. These MERs have be integrated into M-SAPE and used with FIAT as an initial estimate of required material thickness to speed up sizing estimates. When using these MERs, care needs to be taken so that sizing environments, such as peak heating, are within the capabilities of the material.

Acknowledgments

The authors gratefully acknowledge the support provided by the Thermal Protection Materials and Systems Branch and the Reacting Flow Environments Branch of NASA Ames Research Center, through NASA Contract No. NNA10DE12C to the ERC Corporation. Special thanks also go to Richard Winski for supplying the 840 trajectories covering the trajectory space considered for this work.

References

[1] Samareh, J. A., Glaab, L., Winski, R. G., Maddock, R. W., Emmett, A. L., Munk, M. M., Agrawal, P., Sepka, S., Aliaga, J., Zarchi, K., Mangini, N., Perino, S., Bayandor, J., Liles, Charles, "Multi-Mission System Analysis for Planetary Entry (M-SAPE) Version 1," NASA/TM-2014-218507, Aug. 2014.

[2] Wright, M.W., White, T., and Mangini, N., Data Parallel Line Relaxation (DPLR) Code User Manual Acadia Version 4.01.1, NASA/TM-2009-215388, October 2009.

[3] Gnoffo, P. A., "An Upwind-Biased, Point-Implicit Relaxation Algorithm for Viscous, Compressible Perfect-Gas Flows," NASA TP 2953, 1990

[4] Chen, Y.-K., and Milos, F. S., "Fully Implicit Ablation and Thermal Analysis Program (FIAT)," Journal of Spacecraft and Rockets,Vol. 36, No. 3, pp 475-483, May–June 1999

[5] Moyer, C. B., and Rindal, R. A., "An Analysis of the Coupled Chemically Reacting Boundary Layer and Charring Ablator – Part II. Finite Difference Solution for the In-Depth Response of Charring Materials Considering Surface Chemical and Energy Balances", NASA CR-1061, 1968.

[6] Amar, A.J., Calvert, N.D., and Kirk, B.S., "Development and Verification of the Charring AblatingThermal Protection Implicit System Solver" AIAA paper 2011-144, presented at: 49th AIAA Aerospace Sciences Meeting including the New Horizons Forum and Aerospace Exposition, 4 - 7 January 2011, Orlando, Florida

[7] Curry, D. M., "An Analysis of a Charring Ablation Thermal Protection System", NASA TN D-3150, November 1, 1965.

[8] Sutton, K., Graves, R.A., "A General Stagnation-Point Convective Heating Equation For Arbitrary Gas Mixtures" NASA TR R-376, November 1971.

[9] Tauber, M.E., Sutton, K., "Stagnation-Point Radiation Heating Relations for Earth and Mars Entries" AIAA Journal of Spacecraft, Vol. 28, No. 1.

[10] Hui, T., Johnson, C., Rasky, D., Hui, F., Hsu, M., Chen, Y-K., "Phenolic Impregnated Carbon Ablators (PICA) For Discovery Class Mission",NASA Tech Briefs AIAA paper 1996-1911, presented at 31st AIAA Thermophysics Conference, New Orleans, LA, June, 1996.

[11] Clements, H.R. and Ward, G.T., "Fabrication of Ablative Liners for Large Solid Booster Nozzles", J. SPACECRAFT VOL. 3, NO. 4, April 1966

[12] Tran, H.; Johnson, C.; Rasky, D.; and Hui, F. "Silicone Impregnated Reusable Ceramic Ablators for Mars Follow-on Missions", AIAA Paper 96-1819, June 1996.

[13] Edquist, Karl T.; Dyakonov, Artem A.; Wright, Michael J.; Tang, Chun Y., "Aerothermodynamic Design of the Mars Science Laboratory Backshell and Parachute Cone" 41st AIAA Thermophysics Conference; 22-25 Jun. 2009; San Antonio, Texas; United States, AIAA Paper 2009-4078.

[14] Squire, T., Milos, F., Agrawal, P., "Analytical Predictions of Thermal Stress in the Stardust PICA Heatshield Under Reentry Flight Conditions", National Space and Missile Materials Symposium, 28 Jun. - 1 Jul. 2009, Scottsdale, AZ, USA

[15] Milos, F.S., Chen, Y.K., "Two-Dimensional Ablation, Thermal Response, and Sizing Program for Pyrolyzing Ablators", AIAA paper 2008-1223, 46th AIAA Aerospace Sciences Meeting and Exhibit, 7 - 10 January 2008, Reno, Nevada.

[16] Park, C., "Calculation of Stagnation-Point Heating Rates Associated with Stardust Vehicle" AIAA paper 2005-190, 43rd AIAA Aerospace Sciences Meeting and Exhibit, January 2005, Reno, Nevada